High Resolution Exponential Modeling of Fully Polarized Radar Returns

WILLIAM M. STEEDLY, Student, IEEE
RANDOLPH L. MOSES, Senior Member, IEEE
The Ohio State University

A method for modeling full polarization radar targets is considered. The approach taken is to estimate a set of target features which describes the target as a set of attributed scattering centers. Each scattering center is characterized by its range, amplitude, and a polarization ellipse. An exponential model for the fully polarized radar return is described, and an algorithm for estimating the parameters in this model is developed. The modeling procedure is applied to compact range measurements of model aircraft.

Manuscript received January 11, 1990; revised July 2 and July 24, 1990.

IEEE Log No. 44361.

This work was supported in part by the Office of Naval Research under Contract N00014-87-K-2011, and in part by the Air Force Office of Scientific Research, Bolling Air Force Base, Washington, DC.

Authors' address: Dept. of Electrical Engineering, The Ohio State University, 2015 Neil Ave., Columbus, OH 43210.

I. INTRODUCTION

The processing of fully polarized radar target scattering data in order to gain more information about the target is considered. Presently the capabilities of most operational radar systems are limited to the detection of an aircraft and the determination of its position and velocity. It is of interest to gain more information about the physical structure of the radar target for the purpose of identifying the target.

To arrive at the goal of determining such information, this paper considers a method for modeling of radar target signatures from a set of full polarization stepped frequency measurements of the target. Many ways of processing stepped frequency radar measurements have been developed [1–10]. Here, the target signature is modeled using a full polarization exponential model, which characterizes the target as a set of scattering centers each parameterized by its range, amplitude, and polarization ellipse.

One application of this exponential modeling procedure is the automatic target recognition (ATR) problem. A block diagram of an ATR system is shown in Fig. 1. In this system, measurements of known targets are processed into a set of feature vectors θ_i, where each vector describes a target class. This catalog of feature vectors is stored for use in classification. In the operation stage, measurements of an unknown target are processed to obtain an estimated feature vector $\hat{\theta}$. This estimated feature vector is compared with the catalog, and the "closest" match is found to identify the target. In this paper we address the signal processing block of the ATR system in Fig. 1.

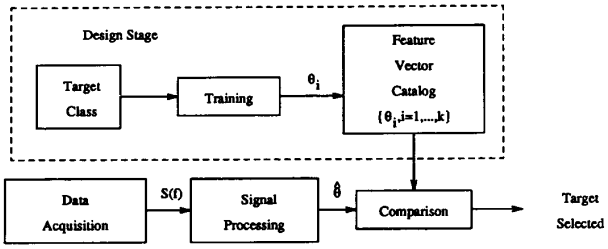

Fig. 1. ATR problem.

The signal processing operation has a major impact on the performance of the ATR system, and is the focus of this work. One desires a feature vector $\hat{\theta}$ which is small in dimension (to keep the computational requirements of the classifier at a modest level), but at the same time has little or no information loss as compared with the original measurements. In addition, the features in $\hat{\theta}$ should be robust to effects of noise, clutter, and small changes in target orientation.

One choice of the feature vector is the direct, stepped frequency scattering measurements. One

can apply parametric or nonparametric statistical decision theory techniques to this feature vector [1, 3, 4]. However, working directly in the frequency domain can have disadvantages. For example, in a wideband radar system, many frequencies may be used, so the length of the feature vector may be prohibitively large, making the classification procedure computationally intensive. Also, this feature vector is sensitive to changes in target orientation, and to changes in target configuration (such as the addition of stores).

Another approach (and the one considered here) is to estimate a time domain feature vector which describes the target. The advantages of time domain characterizations are that the target can be modeled as a relatively small number of scattering centers (thus reducing the dimension of the feature vector) and that these scattering centers have a direct physical interpretation. This idea has been used for some time for single polarization measurements; the approach is to locate scattering centers either by taking the fast Fourier transform (FFT) of the frequency measurements and locating the peaks [2], or by using parametric models, such as autoregressive or autoregressive moving average models, to parameterize the peak response profile [2, 6, 7].

When multiple polarization measurements of a target are available, polarization properties of the targets can also be used as features. Several authors have considered the importance of polarization effects of a target [8–14]. In [8–10] a new way to examine full polarization data is presented; this method provides a description of the interaction of a target with an incident radar wave using the concept of a transient polarization response (TPR). In the TPR concept, the target is illuminated with an impulse of circularly polarized radiation; as the circularly polarized electromagnetic pulse impinges on each scatterer on the target, the scatterer interacts with the pulse and reflects a wave back with a polarization which is determined by the configuration of that scatterer [8–10]. The leading edge of a wing, for example, could be expected to return a horizontally polarized wave if it were illuminated from a nose-on aspect angle with no roll. This type of analysis provides a more complete and descriptive representation of the target than can be obtained from a single polarization signature. Thus, scattering centers are characterized by range, energy, and their polarization effects on a circularly polarized incident wave, which are in general elliptical. In reality a target is not a finite sum of discrete scattering centers but rather has a continuous TPR; thus the TPR is examined where it has high energy content and a scattering center (along with its polarization ellipse) is assigned to that point in the down range.

Nonparametric techniques for extracting scattering centers and their corresponding elliptical polarization returns have been developed in [8–10]. The technique entails taking the FFT of the full polarized, stepped frequency scattering data to form a transient response profile. Scattering centers are estimated by fitting ellipses to the high amplitude portions of this profile. The amplitude and orientation (ellipticity and tilt) of each ellipse is used to characterize the polarization features of each scattering center.

This paper extends the work in [8, 10] by developing a full polarization parametric model of the transient polarization response. This model provides a higher resolution and a reduced set of data with which to identify a target. This offers some advantages over the nonparametric technique in [8, 10]. First, scattering center ranges and polarization ellipses are directly estimated; this eliminates the need for the ellipse-fitting scattering-center extraction step used in the nonparametric method. Second, the parametric technique is capable of higher resolution than the FFT-based method, and can resolve closely spaced scattering mechanisms which the FFT-based methods cannot resolve. This latter point is important for small bandwidth radar applications. It is also important in high fidelity scattering analysis of objects, where one wishes, for example, to separate a direct scattering component from a closely spaced creeping wave component.

In Section II the full polarization, exponential data model is introduced, and a procedure to find ranges and polarization ellipses from the model parameters is outlined. Section III presents an algorithm for finding the parameters of the exponential model from scattering data. Section IV presents simulation results from a simulated model, a simplified aircraft model, and scale models of five commercial aircraft. Finally, Section V concludes the paper.

II. EXPONENTIAL PARAMETRIC MODEL OF TARGET SIGNATURES

Assume we are given a set of full polarization scattering coefficients which are measured from a target at a set of stepped frequencies f_n, $n = 1,2,\ldots,N$ (see [3] for details). We denote these coefficients as $s_{hh}(f)$, $s_{vh}(f) = s_{hv}(f)$, and $s_{vv}(f)$, where the first subscript corresponds to the receive polarization and the second subscript corresponds to the transmit polarization.

The inverse Fourier transform of each set of scattering coefficient data $\{s_{xy}(f_n)\}_{n=1}^{N}$ gives a time or down range impulse response of the target for that polarization [2]. The FFT is often used to compute the impulse response from the scattering data. Various scattering mechanisms will affect the various returns and appear as impulsive responses in the range domain. If these returns are coherent, then scattering mechanisms will appear in one or more polarization returns, and cause impulsive responses at the same range in the range domain. In this way the sets of data can be used together to identify scattering centers.

The polarization properties of each scattering center can be more clearly seen by considering the horizontal and vertical responses to a circularly polarized transmit signal. Left circular has been arbitrarily chosen since, on a macroscopic level, the features of a target appear the same to both left and right circularly polarized transmit fields. In the frequency domain, these scattering coefficients are denoted as $s_{hl}(f_n)$ and $s_{vl}(f_n)$, respectively. These scattering coefficients can be obtained from the horizontal-vertical scattering coefficients using the following transformation [8, 10]:

$$\begin{bmatrix} s_{hl}(f_n) \\ s_{vl}(f_n) \end{bmatrix} = \begin{bmatrix} s_{hh}(f_n) & s_{hv}(f_n) \\ s_{vh}(f_n) & s_{vv}(f_n) \end{bmatrix} \begin{bmatrix} 1 \\ j \end{bmatrix} \frac{1}{\sqrt{2}}. \quad (1)$$

The so-called TPR is found from the inverse Fourier transforms $s_{hl}(r)$ and $s_{vl}(r)$ of the scattering coefficients $s_{hl}(f_n)$ and $s_{vl}(f_n)$. Specifically, the TPR is the plot of the curve $(s_{hl}(r), s_{vl}(r))$ as a function of range r. This curve has the appearance of a set of smoothed, connected ellipses as a function of range, where each ellipse corresponds to a scattering center on the target [10, 8].

In the frequency domain, the TPR can be modeled as

$$\begin{bmatrix} s_{hl}(f_n) \\ s_{vl}(f_n) \end{bmatrix} = \sum_{k=1}^{M} \begin{bmatrix} a_{hk} \\ a_{vk} \end{bmatrix} p_k^n, \qquad n = 1,\ldots,N. \quad (2)$$

Here it is assumed that there are M scattering centers. Each p_k in (2) is a "pole" of the model, and corresponds to a scattering center on the target; the argument of the pole corresponds to the range of the scattering center, and the magnitude of the pole corresponds to the range dispersion of the scatterer. The amplitudes a_{hk} and a_{vk} are the (complex-valued) horizontal and vertical amplitudes, respectively, associated with the kth scattering center. These amplitudes give the polarization properties of each scattering center. For an ideal point scatterer $|p_k| = 1$, but for more realistic targets it is useful to assume that the scattering will be attenuated slightly as frequency either increases or decreases, so $|p_k|$ will vary a little bit around one.

The inverse Fourier transform of (2) gives the impulse response vector

$$\begin{bmatrix} s_{hl}(r) \\ s_{vl}(r) \end{bmatrix} = \sum_{k=1}^{M} \begin{bmatrix} a_{hk} \\ a_{vk} \end{bmatrix} \frac{1}{e^{-j2\pi r/R} - p_k}, \qquad 0 \le r \le R \quad (3)$$

where R is the maximum unambiguous range; R given by $R = c/2\Delta f$ for propagation velocity c and frequency step Δf. It can be seen from (3) that each pole causes a peak in the TPR for ranges (times) at which the incident wave is reflected. Thus, the ranges of these scattering centers are related to the angles of the poles located; if $\angle p_k$ denotes the angle of the kth pole, then the (relative) range of the scattering center is given by

$$r_k = R\frac{\angle p_k}{2\pi}. \quad (4)$$

The fact that the angle of a pole can only be between 0 and 2π rad corresponds to an unambiguous range of R.

The horizontal and vertical amplitudes associated with each pole contain the information about polarization characteristics of each scattering center. These response polarizations are in the form of an ellipse. For each scattering center, the tilt τ_k and ellipticity ϵ_k of this ellipse can be found from the following equations [8, 15]:

$$\tau_k = \tfrac{1}{2}\tan^{-1}[\tan(2\gamma_k)\cos(\delta_k)] \quad (5)$$

$$\epsilon_k = \frac{1}{2}\sin^{-1}(\sin(2\gamma_k)\sin(\delta_k)) \quad (6)$$

$$\gamma_k = \tan^{-1}\left(\frac{|a_{vk}|}{|a_{hk}|}\right) \quad (7)$$

$$\delta_k = \angle a_{vk} - \angle a_{hk}. \quad (8)$$

The above calculations lead to use of only one quarter of the Poincaré polarization sphere. To avoid this ambiguity, the following alterations to the tilt need to be made [8]:

$$\tau_k = \begin{cases} \tau_k + \dfrac{\pi}{2} & \text{if } \gamma_k > \dfrac{\pi}{4} \\ \tau_k + \pi & \text{if } \gamma_k \le \dfrac{\pi}{4} \text{ and } \tau_k < 0. \end{cases} \quad (9)$$

The major axis A_k of each ellipse can be determined as [8, 15]

$$A_k = \left||a_{hk}|\cos(\tau_k) + |a_{vk}|e^{j\delta_k}\sin(\tau_k)\right|. \quad (10)$$

This set of parameters $\{r_k, A_k, \epsilon_k, \tau_k;\ k = 1,\ldots,M\}$ provides a concise description a target. This parameter set characterizes a target as a set of M scattering centers, each described by range, amplitude, and ellipticity and tilt of a scattering polarization ellipse. If used in an ATR system, this set of parameters would form the feature vector θ_i for each catalog entry.

III. ESTIMATING EXPONENTIAL PARAMETRIC MODEL FROM DATA

This section presents an algorithm for estimating the model parameters in (2)–(10) from scattering center data. The algorithm consists of three steps. First, the poles are estimated using linear prediction. Next, the amplitude terms are estimated using a least squares technique. Finally, the amplitude terms are converted into polarization ellipse parameters which describe the polarization ellipse of each scattering center.

The first two steps involve estimating the poles and amplitudes of a damped exponential model. This

problem has been well studied in the time series analysis literature [16, 17], and successful algorithms for single polarization data have been developed [7]. The algorithm below represents a generalization of the one in [7] for the full polarization data case.

First, the poles are estimated using backward linear prediction coupled with least squares [16–18]. The backward linear prediction equations can be written as follows:

$$\begin{bmatrix} s_{hl}(1) & s_{hl}(2) & s_{hl}(3) & \cdots & s_{hl}(L+1) \\ s_{hl}(2) & s_{hl}(3) & & & \vdots \\ \vdots & \vdots & & & \vdots \\ s_{hl}(N-L) & s_{hl}(N-L+1) & \cdots & \cdots & s_{hl}(N) \\ s_{vl}(1) & s_{vl}(2) & s_{vl}(3) & \cdots & s_{vl}(L+1) \\ s_{vl}(2) & s_{vl}(3) & & & \vdots \\ \vdots & \vdots & & & \vdots \\ s_{vl}(N-L) & s_{vl}(N-L+1) & \cdots & \cdots & s_{vl}(N) \end{bmatrix} \times \begin{bmatrix} 1 \\ \hat{b}_1 \\ \vdots \\ \hat{b}_L \end{bmatrix} = 0 \tag{11}$$

or

$$S \begin{bmatrix} 1 \\ \hat{b} \end{bmatrix} = 0 \tag{12}$$

where L is the order of prediction, and $\hat{b}$ is the coefficient vector of the polynomial $\hat{B}(z)$ given by

$$\hat{B}(z) = 1 + \hat{b}_1 z^{-1} + \cdots + \hat{b}_L z^{-L}. \tag{13}$$

Ideally, L can be any integer greater than or equal to the model order M; in practice, choosing $L > M$ results in more accurate parameter estimates. Note that both $s_{hl}(f)$ and $s_{vl}(f)$ are used simultaneously to estimate a single set of prediction coefficients (and therefore, a single set of scattering centers).

The solution of (11) involves obtaining a singular value decomposition of the matrix S and truncating all but the first M singular values to arrive at a noise cleaned estimate $\hat{S}$ [18]. Next, the linear prediction coefficient vector $\hat{b}$ is found as the minimum norm solution of $\hat{S}\begin{bmatrix} 1 \\ \hat{b} \end{bmatrix} = 0$, which is

$$\hat{b} = -\hat{S}_2^{+} \hat{s}_1 \tag{14}$$

where $\hat{s}_1$ is the first column of $\hat{S}$, $\hat{S}_2$ is the remaining L columns of $\hat{S}$, and $^{+}$ denotes the Moore–Penrose pseudoinverse. Finally, the estimated poles are found by

$$\hat{p}_i = \frac{1}{\text{zero}_i\left(\hat{B}(z)\right)}, \qquad i = 1, \ldots, L.$$

Since scattering centers result in peaky responses, those poles which do not lie within a given annular region about the unit circle can be eliminated from the model. The following criterion has been found to work well for radar data [7]:

$$\frac{1}{100} < |\hat{p}_i|^N < 100. \tag{15}$$

This criterion discards any scattering centers whose response energy differs by more than 40 dB from the lowest to highest measured frequency. Poles which do not satisfy (15) are discarded.

Once these poles have been determined, the amplitude equations for both the horizontal and vertical components can be formed. From (2),

$$\begin{bmatrix} \hat{p}_1^1 & \hat{p}_2^1 & \cdots & \hat{p}_{L'}^1 \\ \hat{p}_1^2 & \hat{p}_2^2 & \cdots & \hat{p}_{L'}^2 \\ \vdots & \vdots & & \vdots \\ \hat{p}_1^N & \hat{p}_2^N & \cdots & \hat{p}_{L'}^N \end{bmatrix} \begin{bmatrix} \hat{a}_{h1} & \hat{a}_{v1} \\ \vdots & \vdots \\ \hat{a}_{hL'} & \hat{a}_{vL'} \end{bmatrix} = \begin{bmatrix} s_{hl}(1) & s_{vl}(1) \\ s_{hl}(2) & s_{vl}(2) \\ \vdots & \vdots \\ s_{hl}(N) & s_{vl}(N) \end{bmatrix} \tag{16}$$

or

$$\hat{P}\hat{A} = S_a. \tag{17}$$

Here, L' is the number of poles which satisfy the criterion in (15). The amplitudes can be found from a least squares solution to (17),

$$\hat{A} = \left(\hat{P}^H \hat{P}\right)^{-1} \hat{P}^H S_a. \tag{18}$$

Because only M singular values of $\hat{S}$ are nonzero, there are at most M pole estimates which can correspond to scattering centers on the target. Therefore, only the M poles whose scattering ellipses have the largest energy are retained.

IV. SIMULATION RESULTS

This section presents results obtained by applying the exponential modeling algorithm to various sets of data. First, a simulated point-scattering model of data is used. Next, the algorithm is applied to compact range measurements of a simplified aircraft model. Finally, results using compact range measurements of scale models of five commercial aircraft are presented.

Simulated Point Scatterer Model

In this experiment, we generated scattering data which corresponds to an ideal point scatterer model of an aircraft as shown in Fig. 2. This model, proposed

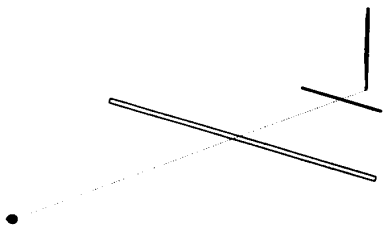

Fig. 2. Ideal point-scattering model.

TABLE I
Ideal Model Data Equations

Scatterer	$\begin{bmatrix} s_{hh}(f) & s_{hv}(f) \\ s_{vh}(f) & s_{vv}(f) \end{bmatrix}$
Nose	$\begin{bmatrix} 1 & 0 \\ 0 & 1 \end{bmatrix} e^{-j4\pi 7.38 f/c}$
Wing	$\begin{bmatrix} \cos^2(10°) & \frac{\sin(20°)}{2} \\ \frac{\sin(20°)}{2} & \sin^2(10°) \end{bmatrix} 10e^{-j4\pi 16.3 f/c}$
Stabilizer	$\begin{bmatrix} \cos^2(10°) & \frac{\sin(20°)}{2} \\ \frac{\sin(20°)}{2} & \sin^2(10°) \end{bmatrix} 2e^{-j4\pi 22.3 f/c}$
Tail	$\begin{bmatrix} \sin^2(10°) & -\frac{\sin(20°)}{2} \\ -\frac{\sin(20°)}{2} & \cos^2(10°) \end{bmatrix} 3e^{-j4\pi 22.6 f/c}$

in [8], consists of four scattering centers located at the nose, wing tips, horizontal stabilizers, and tail. The ranges of the scattering centers are at 0.00, 8.92, 14.9, and 15.2 cm down range with respect to the nose as shown in Fig. 2. The scattering response for the nose is circular, and is linear for the other three scatterers. The aircraft was rolled 10°, so, for example, the wing scattering response is linearly polarized at a 10° angle. The full polarization scattering matrix ($s_{hh}(f)$, $s_{hv}(f) = s_{vh}(f)$, and $s_{vv}(f)$) for each frequency between 2 and 18 GHz in 50 MHz steps was generated by adding the responses for each scatterer as given in Table I.

The horizontal and vertical scattering data was converted to a left circularly polarized transmit basis using (1). The resulting scattering data was applied to the exponential modeling algorithm using $L = 10$ with the following modification. In order to keep the unambiguous range R near the target size, the frequency spacing between measurements should be about 500 MHz, not 50 MHz. To obtain this frequency spacing, the scattering data is decimated by a factor of 10 before processing; for details, see [19]. Exponential models were obtained for model orders $M = 4$ and $M = 3$; these results are summarized by Table II, and portrayed graphically in Figs. 3 and 4.

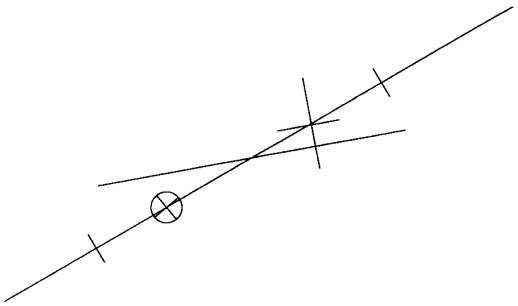

Fig. 3. Ideal model scatterers and polarizations, model order $M = 4$.

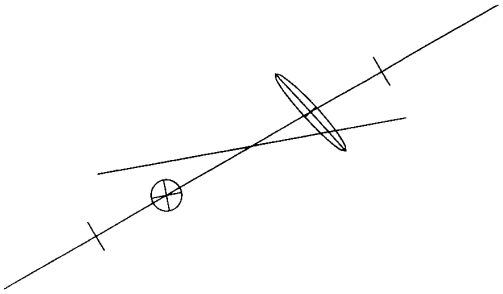

Fig. 4. Ideal model scatterers and polarizations, model order $M = 3$.

The results of the modeling for $M = 4$ are shown in Fig. 3. In this figure, the range axis is the diagonal line, with the unambiguous range denoted by the two tick marks. Each scattering center is shown by an ellipse, and the ellipse graphically describes the amplitude, ellipticity, and tilt of the scattering center. The amplitudes and ellipses in this and all other figures are linearly (not logarithmically) scaled. It can be seen that the four scattering centers are accurately estimated. Moreover, the amplitude and polarization of each scattering center are also estimated very accurately (see also Table II). Note that the horizontal stabilizer and tail are too close in range to be resolved by Fourier-based methods [8]; however, with the exponential modeling method these two scattering centers can be resolved.

If the number of scattering centers in the model is reduced to $M = 3$, then only three scattering centers can be identified, as is shown in Table II and Fig. 4. The nose and wing scattering centers are accurately estimated as before, but now the tail-horizontal stabilizer region is modeled as a single scattering center. Note that the polarization ellipse of the tail region is what one might expect for a combination of the two linearly polarized tail region responses. This example shows that even when the number of scattering centers in the data exceeds the model order, the algorithm generates an estimate which combines closely spaced scattering centers into a conglomerate one. This is an important and desirable characteristic of the algorithm, as radar targets often contain a large

TABLE II
Ideal Model Parameters

Scat.	True Value				M=4 Estimate				M=3 Estimate			
	$\tau(°)$	$\epsilon(°)$	A	r(cm)	$\hat{\tau}(°)$	$\hat{\epsilon}(°)$	$\hat{A}$	$\hat{r}$(cm)	$\hat{\tau}(°)$	$\hat{\epsilon}(°)$	$\hat{A}$	$\hat{r}$(cm)
Nose	-	45.0	.707	7.38	119	45.0	.707	7.38	100	44.1	.718	7.38
Wing	10.0	0.00	7.07	16.3	10.0	0.00	7.07	16.3	10.1	-0.04	7.10	16.3
Stab.	10.0	0.00	1.41	22.3	10.0	0.00	1.41	22.3	131	8.13	2.40	22.5
Tail	100	0.00	2.12	22.6	100	0.00	2.12	22.6				

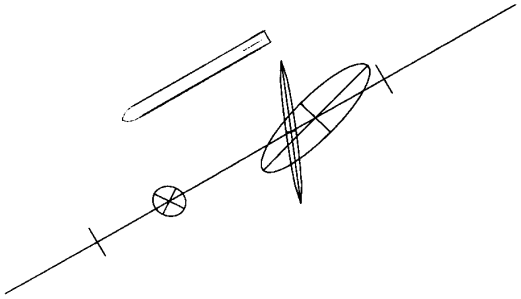

Fig. 5. Scatterers and polarizations for fuselage and tail of simplified aircraft.

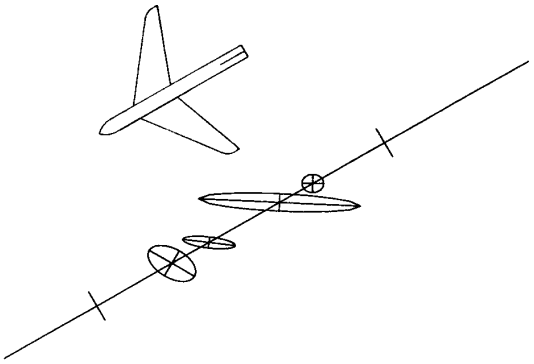

Fig. 6. Scatterers and polarizations for fuselage, wings, and tail of simplified aircraft.

number of scattering centers, not all of which can be individually estimated.

Simplified Aircraft Measurements

Next, the exponential modeling procedure was applied to compact range measurements of a simplified, reconfigurable aircraft target 6 in (15.24 cm) in length. This target consists of a cylindrical fuselage (F) with removable wings (W), horizontal stabilizers (S), and tail (T). Compact range measurements of this model were taken with various parts removed (see [8, 20] for details of the measurement procedure). Each data set consists of full polarization measurements at frequencies between 2 and 18 GHz in 50 MHz steps at a nose-on aspect angle with no roll. The data was decimated by a factor of 10 when applied to the exponential modeling algorithm. The model order L was 10, and the number of singular values kept varied from 3 to 7 depending on the complexity of the target.

Figs. 5–7 show the estimated scattering responses for three configurations of the aircraft. Note that the estimated scattering centers correspond well to target geometry. From these figures it can be seen that the nose scattering is accurately estimated as a nearly circularly polarized response. The two scattering responses at the end of the fuselage-tail configuration in Fig. 5 correspond to the leading and trailing edge of the tail; note the strong vertical polarization of the leading edge, and the more circularly polarized trailing edge response. The trailing edge response is most likely a combination of the tail trailing edge and the cylindrical trailing edge. In Fig. 7 it can be seen that all five scattering center ellipses correspond well with target geometry. The magnitudes of the last two ellipses are about twice as large in the horizontal direction as in the vertical direction, and this corresponds well to the two horizontal fins and one vertical fin at these locations. Modeling results for other configurations of this target are reported in [19].

Scale Model Aircraft Measurements

In this section, the results of modeling scale models of five commercial aircraft (the Boeing 707, 727, 747, DC10, and Concord) are shown. These models measure from 23 to 43 cm in length. Eighty measurements $s_{hh}(f)$, $s_{hv}(f) = s_{vh}(f)$, and $s_{vv}(f)$ on the scale models are taken for frequencies between 6.45 and 10.4 GHz in 50 MHz steps from a nose-on aspect angle with no roll. Details of these measurements are reported in [20, 21]. The models are scaled between 130 and 200 so these results correspond to measurements in the HF band (30 to 90 MHz) for the full sized aircraft. To achieve an unambiguous range of 75 cm, the data was decimated by four in the estimation procedure. A model order of $L = 10$ was chosen and 5 singular values were kept for all the following simulations.

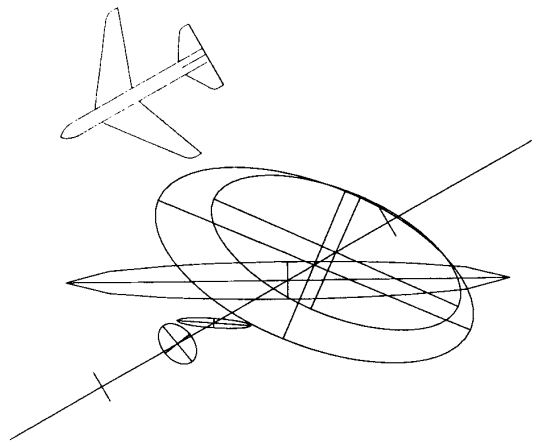

Fig. 7. Scatterers and polarizations for fuselage, wings, stabilizers, and tail of simplified aircraft.

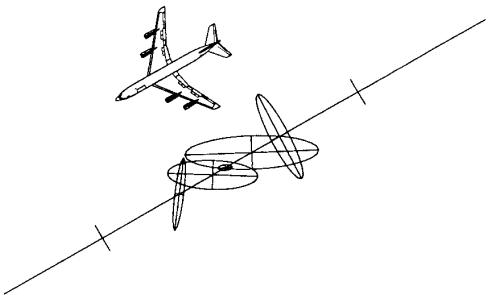

Fig. 8. Boeing 707 scatterers and polarizations.

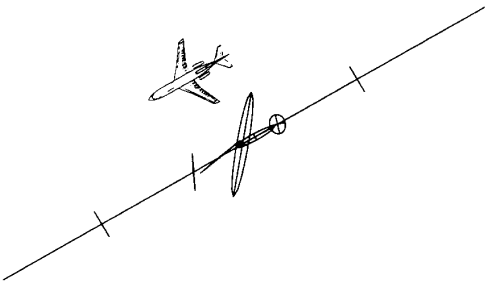

Fig. 9. Boeing 727 scatterers and polarizations.

Figs. 8–12 show the modeling results on the five aircraft models. It can be seen that the cockpit cavity, leading edge of wings, engine inlets, and tail are all located for most of the models. However, unlike the simplified aircraft results, the scattering from the noses of these targets was very small compared with the other scattering centers. The scattering centers and ellipses obtained by the exponential modeling method correlate well with similar nonparametric studies on the same targets as reported in [8–10].

To examine the effects of noise on the estimate, Figs. 13–19 show results of the 707 in 10 and 5 dB

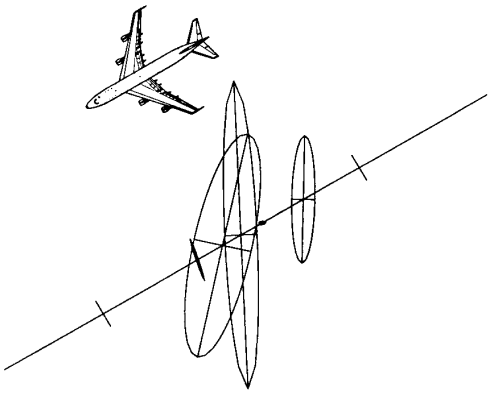

Fig. 10. Boeing 747 scatterers and polarizations.

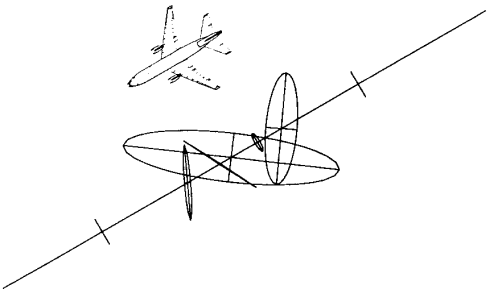

Fig. 11. DC10 scatterers and polarizations.

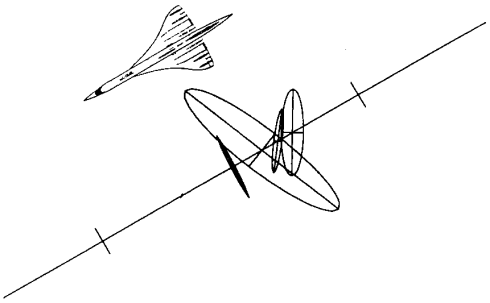

Fig. 12. Concord scatterers and polarizations.

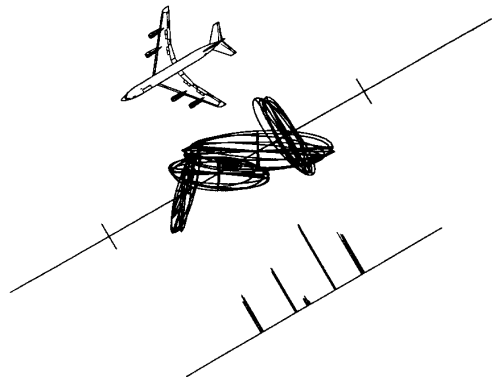

Fig. 13. Boeing 707 scatterers and polarizations, SNR of 10 dB.

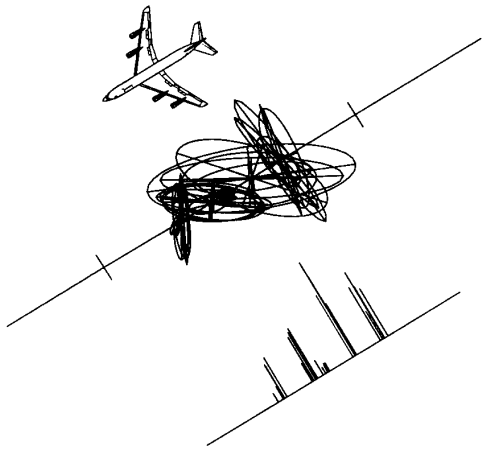

Fig. 14. Boeing 707 scatterers and polarizations, SNR of 5 dB.

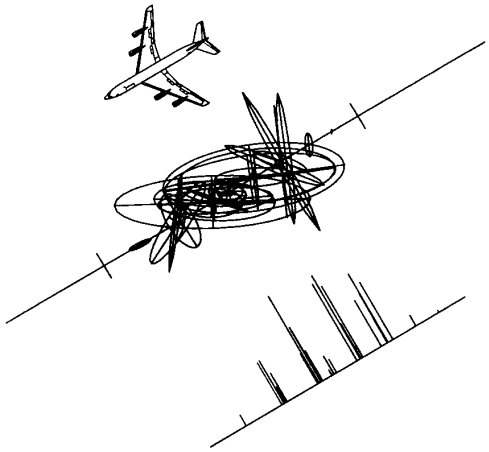

Fig. 15. Boeing 707 scatterers and polarizations, SNR of 0 dB.

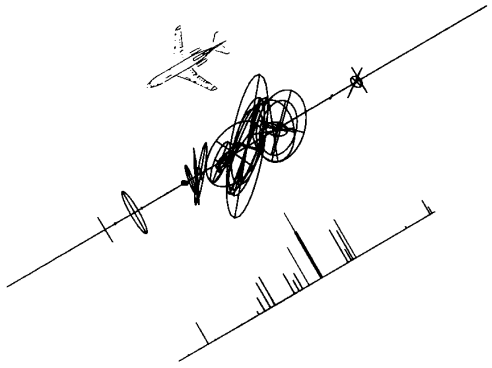

Fig. 16. Boeing 727 scatterers and polarizations, SNR of 0 dB.

signal-to-noise ratio (SNR) and all of the aircraft in 0 dB SNR. In each case, independent white noise was added to each term of the scattering matrix (in left circular coordinates). Five different estimates obtained

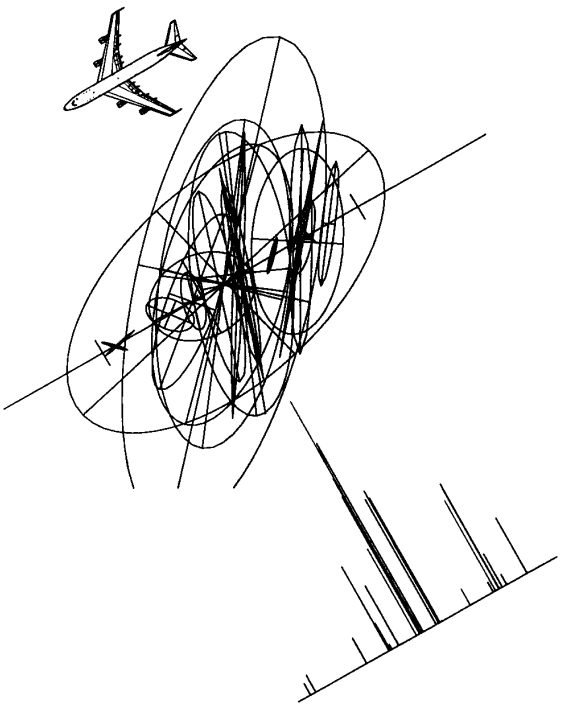

Fig. 17. Boeing 747 scatterers and polarizations, SNR of 0 dB.

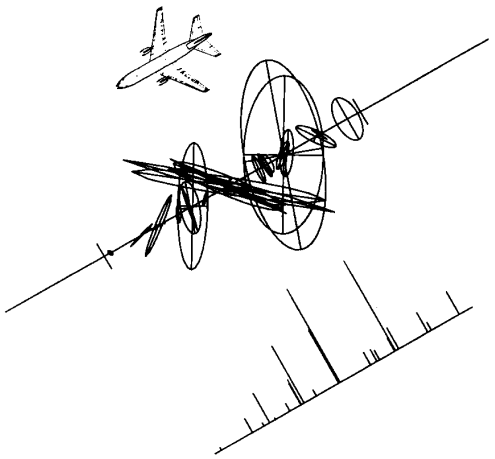

Fig. 18. DC10 scatterers and polarizations, SNR of 0 dB.

from five different noise realizations are shown overlapped in these figures. Two plots of each estimate is shown. The first is the polarization ellipse versus range plot as shown earlier. The second plot shows the magnitude of each ellipse (i.e., the hypotenuse between the major and minor axes) versus range; this plot can be viewed as a projection of the first plot. In the second plot, the tilt angle and ellipticity of the polarization ellipse is lost in the projection. From these figures it can be seen that at 10 dB SNR the estimates show little deviation from the noiseless estimate

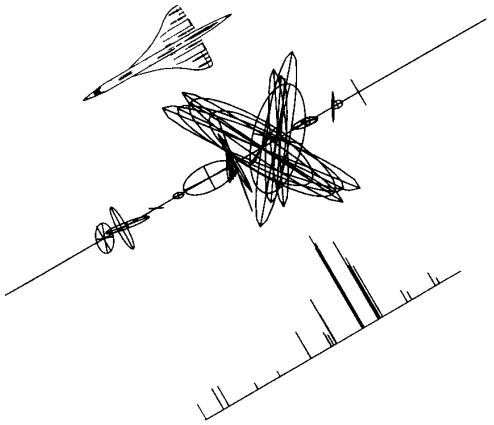

Fig. 19. Concord scatterers and polarizations, SNR of 0 dB.

(compare Fig. 13 with Fig. 8, for example). As the SNR is reduced to 0 dB, the major scattering centers are still estimated; however, the accuracy of the range, amplitude, ellipticity, and tilt decreases somewhat (as is expected). Some spurious estimates are seen but these have small magnitude compared to the actual scattering center magnitudes.

Discussion

The experimental results presented above suggest several characteristics of this full polarization modeling procedure. First, the polarization properties of isolated scattering centers often (but not always) correspond to target geometry. The correspondence was often good for the simplified aircraft target. There were, however, some cases in which the correspondence to geometry was less clear. For example, one might expect the polarization ellipse at the trailing edge of the tail in Fig. 5 to have a tilt angle of 90° instead of 45°.

The correspondence of polarization ellipses with geometry is not as good for the model aircraft; the ranges correspond well with geometry, but the ellipticity and tilt correspond less well. On the other hand, our results are consistent with Fourier-based results as presented in [8–10], so the discrepancies between ellipses and target geometry are not due to modeling errors. We suspect that the cause for this discrepancy is that multiple scattering terms are combined as single scattering centers in both the Fourier-based and the model-based methods. Also, the frequency range of the data is in the resonance region of the target, and scattering contains many interaction terms (creeping waves, multiple interaction scattering, and the like) in this region.

Even when the estimated polarization ellipses do seem to not correspond well with target geometry, the estimates remain stable with respect to noise. In fact, it is encouraging that the algorithm showed a graceful decline in accuracy as the noise power was increased. Of course, our experiments used only white noise; experiments using more realistic noise and clutter need to be performed.

One important advantage of this full polarization technique is that scattering centers of a given cross section are estimated with equal accuracy regardless of their polarization. If, for example, one uses only HH polarization data, scattering centers which are vertically polarized will appear as weak in the HH domain, and may be missed. An example is the Boeing 747 in Fig. 10, where all of the major scattering centers are vertically aligned, so they would appear weaker if only HH data were used to estimate the scattering behavior.

The examples demonstrate that the exponential modeling method is capable of estimating scattering centers and their polarization properties. However, we have not yet addressed the issue of whether or not these features would prove useful as discriminants in an ATR system. There are advantages to using full polarization data; full polarization features provide more information than just amplitude of the single polarization scattering centers, and full polarization data does not miss scattering centers which happen to scatter energy in an orthogonal polarization as single polarization data processing might. Also, preliminary studies on the utility of this polarization information for target identification were reported in [8–10], and polarization information did provide improved target classification in these studies. However, whether these advantages are great enough to outweigh the additional data collection and signal processing effort is an (as yet) unanswered question.

V. CONCLUSIONS

This paper has presented a method of processing full polarization, stepped frequency measurements of a target. A parametric model which describes the target as a set of scattering centers is developed. Each scattering center is characterized by a polarization ellipse, which corresponds to the backscattered polarization ellipse from a circularly polarized incident wave. An estimation procedure to find the parameters of this model is developed. Simulation results are presented for both synthetic data and compact range measurements of aircraft. The results show that the algorithm is capable of identifying scattering mechanisms of the target, and that the estimated polarization ellipse of each scattering center often correlates well with the geometry of the target. The signatures of various aircraft are seen to show such features as wings, engine inlets, cockpit cavity, and tail. Tests using noisy data show that dominant scattering is well estimated even at 0 dB SNR. Current research is focused on using these estimated parameters as feature vectors in an ATR system.

REFERENCES

[1] Ksienski, A. A., Lin, Y. T., and White, L. J. (1975)
Low-frequency approach to target identification.
Proceedings of the IEEE, **63**, 12 (Dec. 1975), 1651–1660.

[2] Mensa, D. L. (1981)
High Resolution Radar Imaging.
Dedham, MA: Artech House, 1981.

[3] Kamis, A., Garber, F. D., and Walton, E. K. (1985)
Radar target classification studies—software development and documentation.
Technical report 716559-1, The Ohio State University, Department of Electrical Engineering, ElectroScience Laboratory, Sept. 1985.

[4] Chen, J. S., and Walton, E. K. (1986)
Comparison of two target classification techniques.
IEEE Transactions on Aerospace and Electronic Systems, **AES-22**, 1 (Jan. 1986), 15–22.

[5] Goh, T. T., Walton, E. K., and Garber, F. D. (1987)
X-band ISAR techniques for radar target identification.
Technical report 717975-1, The Ohio State University, Department of Electrical Engineering, ElectroScience Laboratory, Mar. 1987.

[6] Moses, R. L., and Carl, J. (1988)
Autoregressive modeling of radar data with application to target identification.
In *Proceedings of the IEEE 1988 National Radar Conference*, Ann Arbor, MI, Apr. 20–21, 1988, 220–224.

[7] Carrière, R., and Moses, R. L. (1988)
Autoregressive moving average modeling of radar target signatures.
In *Proceedings of the IEEE 1988 National Radar Conference*, Ann Arbor, MI, Apr. 20–21, 1988, 225–229.

[8] Chamberlain, N. F. (1989)
Recognition and analysis of aircraft targets by radar, using structural pattern representations derived from polarimetric signatures.
Ph.D. dissertation, The Ohio State University, June 1989.
Also: ElectroScience Laboratory report 719710-3.

[9] Garber, F. D., Chamberlain, N. F., and Snorrason, O. (1988)
Time-domain and frequency-domain feature selection for reliable radar target identification.
In *Proceedings of the IEEE 1988 National Radar Conference*, Ann Arbor, MI, Apr. 20–21, 1988, 79–84.

[10] Chamberlain, N. F., Walton, E. K., and Garber, F. D. (1990)
Radar target identification of aircraft using polarization-diverse features.
IEEE Transactions on Aerospace and Electronic Systems, **27**, 1 (Jan. 1991), 58–66.

[11] Copeland, J. R. (1960)
Radar target classification by polarization properties.
Proceedings of the IRE, **48**, 7 (July 1960), 1290–1296.

[12] Boerner, W., El-Arini, M., Chan, C., and Mastoris, P. (1981)
Polarization dependence in electromagnetic inverse problems.
IEEE Transactions on Antennas and Propagation, **AP-29**, 2 (Mar. 1981), 262–271.

[13] Manson, A. C., and Boerner, W. M. (1985)
Interpretation of high-resolution polarimetric radar target down-range signatures using Kennaugh's and Huynen's target characteristic operator theories.
In *Inverse Methods in Electromagnetic Imaging: Part II*, W. M. Boerner (Ed.), Dordrecht, Holland: Reidel, 1985.

[14] Novak, L. M., Sechtin, M. B., and Cardullo, M. J. (1989)
Studies of target detection algorithms that use polarimetric radar data.
IEEE Transactions on Aerospace and Electronic Systems, **AES-25**, 2 (Mar. 1989), 150–165.

[15] Kraus, J. D., and Carver, K. R. (1973)
Electromagnetics.
New York, NY: McGraw-Hill, 1973.

[16] Kay, S. M. (1988)
Modern Spectral Estimation, Theory and Application.
Englewood Cliffs, NJ: Prentice-Hall, 1988.

[17] Marple, L. (1987)
Digital Spectral Analysis with Applications.
Englewood Cliffs: Prentice-Hall, 1987.

[18] Kumaresan, R., and Tufts, D. W. (1982)
Estimating the parameters of exponentially damped sinusoids and pole-zero modeling in noise.
IEEE Transactions on Acoustics, Speech, and Signal Processing, **ASSP-30**, 6 (Dec. 1982), 833–840.

[19] Steedly, W. M. (1989)
High resolution exponential modeling of fully polarized radar returns.
M.S. thesis, The Ohio State University, Oct. 1989. Also: ElectroScience Laboratory report 717220-3.

[20] Walton, E. K., and Young, J. D. (1984)
The Ohio State University compact radar cross-section measurement range.
IEEE Transactions on Antennas and Propagation, **AP-32**, 11 (Nov. 1984), 1218–1223.

[21] Kamis, A., Walton, E. K., and Garber, F. D. (1987)
Radar target identification techniques applied to a polarization diverse aircraft data base.
Technical report 717220-2, The Ohio State University, Department of Electrical Engineering, ElectroScience Laboratory, Mar. 1987.

William M. Steedly (S'86) received the B.S. degree in electrical engineering from Virginia Polytechnic Institute and State University, Blacksburg, in 1988 and the M.S. degree in electrical engineering from The Ohio State University, Columbus, in 1989.

During the 1988–1989 academic year he was an Ohio State University Fellow. Since 1989 he has been an Air Force Laboratory Graduate Fellow in the Department of Electrical Engineering, The Ohio State University. His research interests include parametric modeling techniques and radar signal processing.

Mr. Steedly is a member of Eta Kappa Nu, Tau Beta Pi, and Phi Kappa Phi.

Randolph L. Moses (S'78—M'85—SM'91) received the B.S., M.S., and Ph.D. degrees in electrical engineering from Virginia Polytechnic Institute and State University, Blacksburg, in 1979, 1980, and 1984, respectively.

During the summer of 1983 Dr. Moses was an SCEEE Summer Faculty Research Fellow at Rome Air Development Center, Rome, NY. From 1984 to 1985 he was with the Eindhoven University of Technology, Eindhoven, The Netherlands, as a NATO Postdoctoral Fellow. Since 1985 he has been an Assistant Professor in the Department of Electrical Engineering, The Ohio State University. His research interests are in digital signal processing, and include parametric time series analysis, radar signal processing, system identification, and model reduction.

He is a member of Eta Kappa Nu, Tau Beta Pi, Phi Kappa Phi, and Sigma Xi.